Eur Spine J (2003) 12 : 300–306
DOI 10.1007/s00586-002-0492-9

ORIGINAL ARTICLE

Andrew R. Brodbelt
Marcus A. Stoodley
Amy M. Watling
Jian Tu
Nigel R. Jones

Fluid flow in an animal model of post-traumatic syringomyelia

Received: 25 July 2002
Accepted: 25 July 2002
Published online: 6 December 2002

This research project was supported by grants from the National Health and Medical Research Council of Australia (Project no. 157063), and the Australian Brain Foundation. A R Brodbelt is supported by a grant from the Madeline Foundation for Neurosurgical Research.

A.R. Brodbelt (✉) · M.A. Stoodley
A.M. Watling · J. Tu
Prince of Wales Medical Research Institute,
University of New South Wales,
Barker Street, Randwick,
NSW 2031 Australia
e-mail: abrodbelt@doctors.org.uk,
Tel.: +61-2-9382-2420,
Fax: +61-2-9382-2428

N.R. Jones
Department of Surgery (Neurosurgery),
University of Adelaide, South Australia,
5000 Australia

Abstract More than a quarter of patients with spinal cord injury develop syringomyelia, often with progressive neurological deficit. Treatment options remain limited and long-term failure rates are high. The current poor understanding is impeding development of improved therapies. The source and route of fluid flow into syringes has been investigated using cerebrospinal fluid (CSF) tracers. Previous work using a model of canalicular syringomyelia has shown that fluid enters the dilated central canal from perivascular spaces. The aim of this study was to determine the source and route of fluid flow in an animal model of extracanalicular (post-traumatic) syringomyelia. A model of post-traumatic syringomyelia was established in 25 Sprague-Dawley rats with intraparenchymal injections of quisqualic acid and kaolin-induced arachnoiditis. Rats survived for 6 weeks before injection of the CSF tracer horseradish peroxidase into the cisterna magna. Examination of the spatial distribution of horseradish peroxidase at 0, 3, 5, 10, or 20 min after injection was used to determine the route of fluid flow. Horseradish peroxidase rapidly spread to the ventromedian fissure, perivascular spaces, central canal, and extracanalicular syrinx. Flow occurred into the syrinx prior to significant perivascular flow in the rostral spinal cord. Preferential flow into the syrinx occurred from the perivascular spaces of the central penetrating branches of the anterior spinal artery in the grey matter. Transparenchymal flow into the syrinx was less prominent than perivascular flow. This is the first report of fluid flow within the spinal cord in a model of post-traumatic syringomyelia. Fluid from perivascular spaces moves preferentially into extracanalicular syringes and the surrounding parenchyma. Obstruction to CSF flow and loss of compliance from traumatic arachnoiditis might potentiate fluid flow in the perivascular space.

Keywords Syringomyelia · Animal model · Post-traumatic · Fluid flow · Perivascular space

Introduction

Up to 28% of patients will develop a syrinx after spinal cord injury, and follow-up studies demonstrate that fewer than half will improve following treatment [2, 4, 17, 19, 27, 32, 33, 36, 42]. Development of more effective treatment is unlikely without a better understanding of the underlying aetiology. Most theories of the aetiology of syringomyelia have concentrated on the canalicular type associated with Chiari malformations [3, 11, 14, 25, 40, 44]. To date there have been no adequate explanations of the hydrodynamic forces that produce post-traumatic extracanalicular syringes.

Spinal cord injury can produce a non-communicating extracanalicular syrinx at the site of injury up to 34 years

after the injury [2, 21, 31, 34]. There is often a release of excitotoxic amino acids at the site and time of injury, followed at a later stage by the development of subarachnoid adhesive arachnoiditis [10, 17, 20, 26, 37]. An experimental animal model has been developed that combines excitotoxic amino acid injections with localized arachnoiditis to produce extracanalicular syringes [5, 47, 49].

The aim of the current study was to determine the route of fluid flow into extracanalicular syringes in this new model.

Materials and methods

Following ethical approval from the animal care and ethics committee of the University of New South Wales, 25 Sprague Dawley rats weighing 307–488 g were obtained for the study. Cerebrospinal fluid (CSF) flow was examined in each animal 6 weeks after a syrinx induction procedure.

Syrinx induction

The experimental procedures have been described in detail previously [39, 47]. All procedures were performed in a sterile field under general anaesthetic. Anaesthesia was induced with 4% isoflurane in oxygen and followed with 2.5% isoflurane maintenance, increased if required to maintain an adequate level of anaesthesia. The rats were placed prone, self-ventilating through a nose cone, and the skin was shaved and prepared with povidine-iodine. Local anaesthetic (0.15 ml of 0.5% bupivicaine) was infiltrated into the skin. A T1–C6 laminectomy was performed. The dura was opened and the pia punctured. A glass needle tipped (outside diameter 50 μm) 5 μl syringe (SGE, Australia) held in a stereotactic micromanipulator was used to infiltrate four 0.5-μl injections of 24 mg/ml quisqualic acid and 1% Evans blue. Evans blue allowed any leakage of the quisqualic acid to be identified and corrected. The injections were positioned along the line of entry of the right dorsal nerve rootlets between the rostral C7 rootlets and the caudal C8 rootlets. Ten microlitres of 250 mg/ml kaolin were then injected into the subarachnoid space to produce arachnoiditis. All animals were allowed to recover with appropriate analgesia, and free access to food and water. Any excessive weight loss, limb weakness, or signs of over self-grooming were recorded.

CSF tracer studies

After 6 weeks, the animals were reanaesthetised, and the posterior atlanto-occipital membrane was exposed. A sharpened needle on a 10 μl syringe (SGE) was carefully passed through the atlanto-occipital membrane into the subarachnoid space without loss of CSF. Ten microlitres of 3% horseradish peroxidase (HRP; Zymed Laboratories) in 0.9% sterile saline was injected into the CSF at 2 μl/min for 5 min. The needle was left in place until fixation to prevent leakage. After 0, 3, 5, 10, or 20 min following the end of the HRP injection, the animals were rapidly perfused by intracardiac injection of 5000 IU heparin in 2 ml saline followed by 500 ml of 4% paraformaldehyde in 0.1 M phosphate buffer (pH 7.4) over 15 min. (In two animals a more rapid injection was used (4 μl/min over 2.5 min), and these were perfused immediately thereafter).

Processing

The spinal column and skull were dissected out and post-fixed in 4% paraformaldehyde in 0.1 M phosphate buffer (pH 7.4) overnight. The dura was dissected off the cord, and vibratome sections were taken from cerebral cortex, C2, L2, and serially from C4–T4 for CSF tracer analysis. Paraffin embedded sections from C3, L3 and segments adjacent to or containing a syrinx were also taken for morphological study.

HRP analysis commenced with transverse or sagittal sections of 50 μm cut from each block using a vibratome and floated onto a water bath containing 0.1 M Tris buffer (pH 7.6). Sections were mounted on 3-amino propyl-triethoxy-silane (APT) coated slides, blotted dry, and left to air dry for at least 4 h.

The sections were rinsed for 15 s in distilled water, and then incubated for 20 min in 0.01 M sodium acetate buffer (pH 3.3) containing 0.005% 3,3',5,5' tetramethylbenzidine (TMB; Lancaster Synthesis Ltd, UK) and 0.1% sodium nitroferricyanide (III) dihydrate (Lancaster Synthesis Ltd). The sections were incubated for a further 20 min following the addition of 30 μl of hydrogen peroxide for a final concentration of 0.01%. After washing in 0.01 M sodium acetate buffer (pH 3.3), the slides were transferred to 5% ammonium molybdate (IV) tetrahydrate (Lancaster Synthesis Ltd) in 0.01 M sodium acetate buffer to stabilise the reaction product. Finally, the slides were washed in 0.01 M sodium acetate buffer for 30 s, followed by gradient ethanol baths, xylene and then coverslipped.

Blocks for paraffin embedding were processed using gradient ethanol baths, xylene, and then paraffin. Sections were stained with haematoxylin and eosin for histological comparison to the corresponding HRP-stained spinal cord sections.

Results

All animals developed a noncommunicating extracanalicular syrinx that ranged from one to four segments in length (mean 2.3±SD 0.9 segments). The syringes were situated in the right lateral grey matter, except for two animals where bilateral changes were evident. There was significant neuronal loss at the site of quisqualic acid microinjection, and the syringes were surrounded by gliosis and inflammatory infiltrate. Because the dura was removed to aid sectioning, arachnoiditis was only visible where intact arachnoid remained. One animal was excluded from the study, as it did not survive beyond 24 h of the initial procedure.

HRP staining was evident in the syringes in some animals at each time point, suggesting rapid movement of fluid throughout the spine. The ventromedian fissure was stained in 21 of 24 animals (88%) at all levels or at any level where the perivascular space of the central branches of the anterior spinal artery, central canal, or the syrinx was stained. The ventromedian fissure and peripheral parts of the perivascular space of the penetrating branches of the anterior and posterior spinal arteries were heavily stained in caudal parts of the spinal cord. There was evidence of tracer between the perivascular space of the central branches of the anterior spinal artery and the central canal in 16 of 24 animals (67%) (Fig. 1). The central canal at adjacent levels had tracer present, without staining of all the adjacent perivascular spaces of the central branches of the anterior spinal artery. Although the penetrating branches of the anterior and posterior spinal arteries were stained in most sections, these branches ended in the white matter and seldom demonstrated tracer between them and

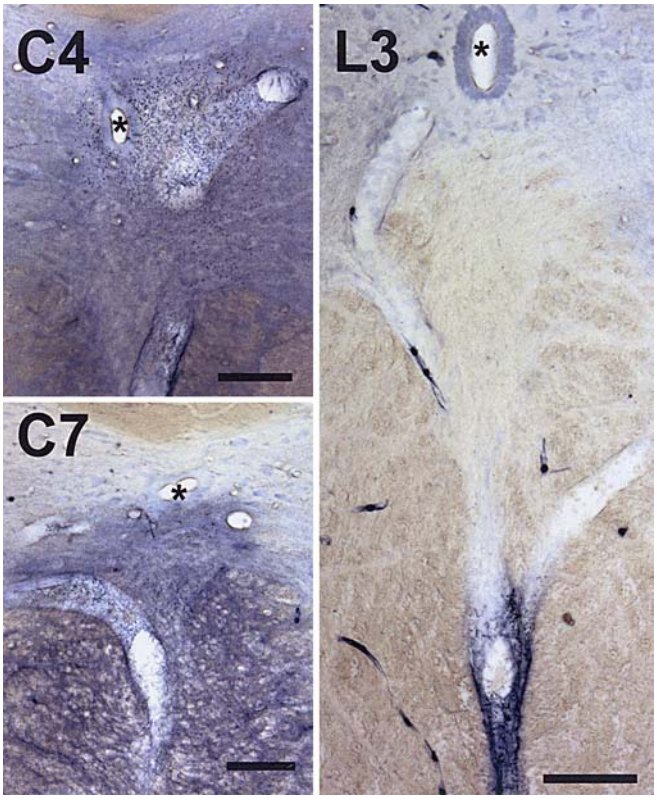

Fig. 1 Tetramethylbenzadine (TMB) stained sections from a single animal fixed immediately after an injection of horseradish peroxidase (HRP) into the cisterna magna. The central canal (*) is uppermost, whilst the ventromedian fissure lies inferiorly. At C4, cerebrospinal fluid (CSF) tracer is present in the perivascular space, central canal, and intervening parenchyma, whilst at C7 the central canal is spared, and at L3 only the ventromedian fissure is stained. This is interpreted as indicating progressive fluid flow down the ventromedian fissure, perivascular space, and into the central canal (*bar* = 100 μm)

the central grey matter. The central canal was dilated in only one animal. Perivascular space dilatation occurred in only one animal. Diffuse pale neuronal background staining was observed in a number of animals.

In seven animals, the syrinx was not stained, and four of these had been fixed immediately after HRP infusion. HRP was present between the central branches of the anterior spinal artery and the syrinx in 14 of the remaining 17 animals (82%) (Fig. 2). There was little evidence of staining between the peripheral penetrating branches of the anterior and posterior spinal arteries and the syrinx cavity, unless the syrinx was large or peripheral. Tracer was present between the subarachnoid space and the syrinx in nine animals (53%) (Fig. 2). Nine animals had heavily stained perivascular space, parenchyma and syrinx compared to much lighter staining at the levels above (Fig. 3). Longitudinal sectioning of syringes revealed diffuse distribution of tracer proximal and distal to the cavity. By 20 min, significant transpial staining (≥200 μm) had occurred, and some cortical neurones and axons were labelled.

Discussion

Syringomyelia may be classified pathologically into communicating central canal syringes, non-communicating central canal syringes and extracanalicular syringes [21]. Post-traumatic and arachnoid adhesion-related syringes are extracanalicular, do not communicate with the central canal, and are lined by gliosis rather than a complete or discontinuous ependymal lining [21, 23]. This contrasts with the Chiari-associated canalicular syringes and suggests a different underlying aetiology.

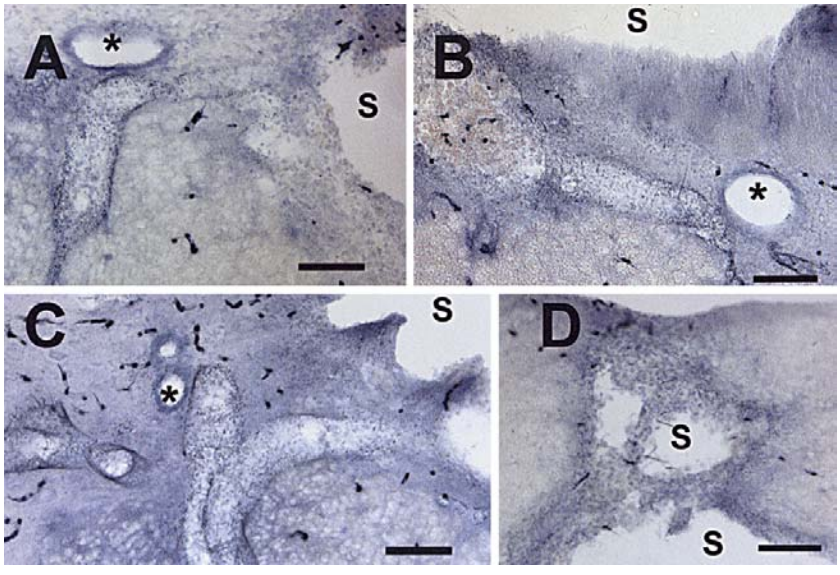

Fig. 2 TMB stained sections indicating CSF tracer in the perivascular space of the central branches of the anterior spinal artery, central canal (*), syrinx (*S*), and intervening parenchyma (**A, B, C**). Some animals demonstrated tracer between the syrinx and the subarachnoid space along the dorsal horn (**D**). The conclusion reached was that most flow into the syrinx arises from the central perivascular space, and that transparenchymal flow may be outflow (*bar* = 100 μm)

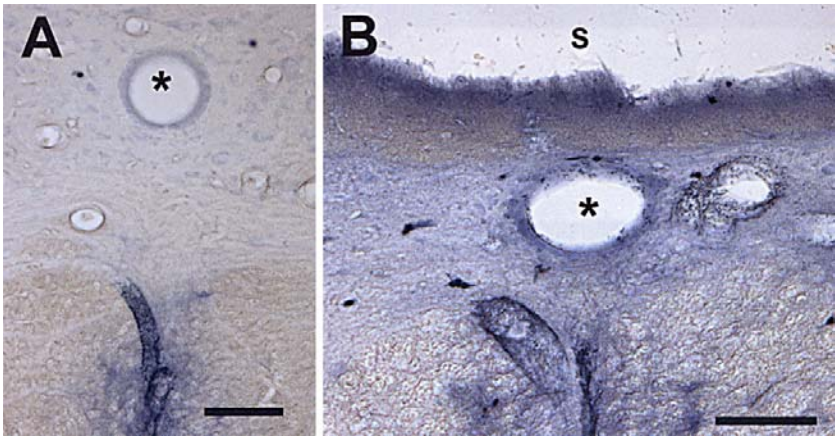

Fig. 3 Sections fixed 20 min after an infusion of HRP at the cisterna magna and stained with TMB. There is much less reaction product at C5 (**A**) than at the level of the syrinx (C8, **B**), suggesting preferential flow into the cord at this level (*asterisk* central canal, *S* syrinx, *bar* = 100 μm)

Animal model

The excitotoxic animal model of post-traumatic syringomyelia mimics the chemical effects of trauma to the cord. Other models rely on the weight drop method of injury, or direct fluid injection to produce an extracanalicular syrinx in a limited number of animals [1, 8, 13, 41, 46]. Excitotoxic amino acids are released at the time of cord injury [20, 26, 37]. Microinjection of quisqualic acid (QA) [an alpha-amino-3-hydroxy-5-methyl-4-isoxazolepropionic acid (AMPA) metabotropic receptor agonist and excitotoxic amino acid] into the spinal cord grey matter in rats produces selective neuronal death, inflammation and the development of a noncommunicating extracanalicular cavity [28, 35, 49]. Combination of intraparenchymal QA with a local injection of subarachnoid kaolin to promote arachnoiditis produces significantly longer and wider syringes than does QA or kaolin alone [47]. Refinement of the experimental techniques has produced a reliable model of posttraumatic syringomyelia that histologically mimics the human disease [5]. The excitotoxic amino acid animal model used in this experiment mimics the distinct histopathology of post-traumatic syringomyelia.

Spinal fluid flow

The route of fluid flow into post-traumatic syringes is unknown. Investigating the route of fluid flow into syringes has proved difficult. Post-mortem injection of ink into the cisterna magna stains perivascular spaces, and tracers injected into syringes reach the cisterna magna, suggesting a pathway between the fluid spaces [3]. Myelography demonstrates inflow into a syrinx within 6 h [16]. Radiolabelled albumin moves from the cortex or cerebral subarachnoid space into the perivascular spaces more rapidly and crosses the pial membrane [7, 15].

Investigations of CSF flow require a fluid tracer; however, the ideal CSF tracer does not exist. HRP has a number of advantages over other tracers. It is a glycoprotein, MW 44 kDa, that is small enough to pass with CSF through normal fluid channels, is large enough not to diffuse, is sensitively labelled with tetramethylbenzadine, and as a protein is anchored in-situ on fixation. In rats, HRP moves within 10 min from the cisterna magna to the perivascular spaces of spinal arteries and on into the central canal [29, 30, 38]. In an animal model of canalicular syringomyelia, HRP moved rapidly into the enlarged central canal in spite of histological evidence of increased pressure [39]. The observed spread of HRP following injection is not due to simple diffusion or as a post-mortem artefact, but is a representation of bulk flow [15, 30, 38].

Examination of the temporal and spatial characteristics of HRP in the spinal cord after microinjection provides evidence for the route of fluid flow. HRP takes time to pass down the spinal subarachnoid space, reaching the conus medullaris last. The pattern of staining in caudal parts of the cord indicated that the ventromedian fissure and PVS of branches of the anterior and posterior spinal arteries were the initial entry points of fluid flow into the cord. We have demonstrated HRP staining of syringes and perivascular spaces in animals fixed rapidly following an HRP injection over 2.5 min. Although the use of tetramethylbenzadine has been criticised as being too sensitive, it does demonstrate that some fluid movement exists, and allows simple conclusions concerning fluid flow to be made [15]. The density of reaction product in these experiments is assumed to be proportional to the rate and amount of fluid flowing into the spinal cord from the subarachnoid space. In addition to the density of reaction product, the number of perivascular spaces stained is indicative of the extent of flow into the cord.

The progressive staining of the ventromedian fissure, followed by the PVS of the central branches of the anterior spinal artery and central canal, suggests progressive flow of fluid down these anterior spinal artery branches as they pass through the ventromedian fissure and on through the cord parenchyma adjacent to the central canal and then into the central canal (Fig. 4). Fluid may run along the

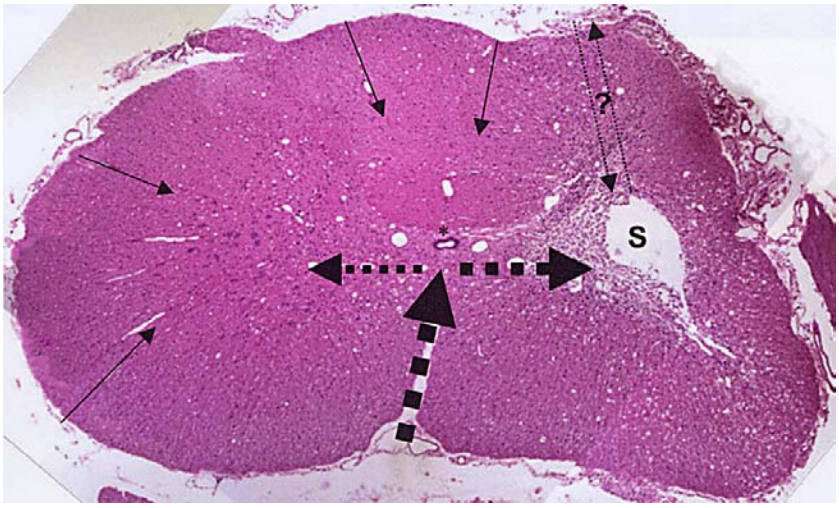

Fig. 4 Haematoxylin and eosin stained section indicating the proposed routes of fluid into the spinal cord and syrinx (*S*). Fluid flows along all the perivascular spaces into the cord, but the main contribution to the central grey matter, central canal (*), and syrinx arises from the central branches of the anterior spinal artery. Transparenchymal flow may be out of the syrinx (?)

central canal for a number of segments. Concomitant inflow of CSF into penetrating branches of the anterior and posterior spinal arteries, as opposed to transpial flow, suggests that the perivascular space of all vessels is the preferential route of fluid flow into the cord. As fluid flow into the cord appears substantial, a continuous circulation of fluid must exist in the spinal cord between the interstitial, perivascular, and subarachnoid fluid spaces. Fluid returning to the subarachnoid space may do so via venous perivascular spaces, but this cannot be confirmed by the current study.

The results of the current study suggest that a continuous flow of CSF occurs down all perivascular spaces into the spinal cord. When a syrinx is present, fluid enters the cavity from the nearest PVS. The central branches of the anterior spinal artery are often the closest vessels to the syrinx, have the largest diameter, and supply the majority of blood to the central grey matter [18]. The role of these perivascular spaces as the major route of fluid influx into the syrinx is therefore not surprising (Fig. 4). The evidence for direct transparenchymal flow, although present, was less compelling.

Why should fluid flow into the cord preferentially at the level of a syrinx? It is unlikely that an intrinsic cord abnormality sucks fluid in when operative evidence in humans suggests that the syrinx is under higher pressure than the surrounding subarachnoid space [9, 24]. A change in the subarachnoid space compliance induced by arachnoiditis or any local deformity might potentiate perivascular fluid flow by reducing access to the expansile lumbar cistern or increasing the fluid propagation effects of local spinal arteries. Mathematical modelling suggests that a pressure wave travelling down the spinal subarachnoid space on reaching an obstruction would rebound into the cord [6]. This elastic jump might work to feed more fluid into a local arterial pumping mechanism. Transparenchymal flow could simply be fluid egress from the syrinx along a route of low resistance.

Syrinx aetiology

The mechanisms of syrinx formation, and route and source of fluid flow following trauma remain unknown. Previous hydrodynamic theories proposed that fluid flowed down the central canal due to arterial or respiratory pressure differentials, followed by rostral canal obstruction leading to a non-communicating syrinx [11, 12, 43]. The theories are difficult to reconcile with the findings that the central canal is largely obstructed in humans by the age of 30, and that there is a clear histological distinction between the central canal and the syrinx cavity in post-traumatic syringomyelia [21, 22, 23, 48]. Haematoma formation at the time of injury has been suggested as creating an initial cavity, with subsequent respiratory pressure differentials on the external cord inducing fluid movement within the cavity, dissecting the cord and propagating the syrinx [45]. There is no experimental or observational evidence to confirm that this induced fluid movement within the cord is powerful enough to cause syrinx enlargement [17]. There is evidence for arterial pulsation-driven perivascular flow as the mechanism of syrinx enlargement in the canalicular type of syringomyelia [39]. The current findings support a similar mechanism for extracanalicular syringes.

Future investigations

Mathematical and biomechanical modelling may contribute to our understanding of spinal fluid flow. The effects of surgical treatments on the route and amount of fluid flow in animal models will provide valuable insights into the underlying mechanisms. Although genetic engineering and stem cell implants may have a therapeutic role in the future, their current uses are limited by our lack of knowledge of the underlying mechanism of syrinx formation.

Conclusions

Investigations in the excitotoxic amino acid model of post-traumatic syringomyelia demonstrated fluid flow from the spinal subarachnoid space into the perivascular spaces of mainly the central branches of the anterior spinal artery and into the central canal or syrinx. Fluid flowed preferentially at the level of the syrinx, suggesting that a change in subarachnoid space compliance potentiates a local arterial-driven perivascular flow. Improved understanding of the mechanism of post-traumatic syringomyelia hopefully will lead to the development of new and improved treatment options.

References

1. Allen AR (1911) Surgery of experimental lesion of spinal cord equivalent to crush injury of fracture dislocation of spinal column. JAMA 57:878–880
2. Backe HA, Betz RR, Mesgarzadeh M, Beck T, Clancy M (1991) Post-traumatic spinal cord cysts evaluated by magnetic resonance imaging. Paraplegia 29:607–612
3. Ball MJ, Dayan AD (1972) Pathogenesis of syringomyelia. The Lancet 2: 799–801
4. Batzdorf U, Klekamp J, Johnson JP (1998) A critical appraisal of syrinx cavity shunting procedures. J Neurosurg 89:382–388
5. Brodbelt AR, Stoodley MA, Brown CJ, Jones NR (2001) Time and dose profiles of experimental excitotoxic post-traumatic syringomyelia (Abstract). Aust N Z J Surg 71:A66
6. Carpenter PW, Berkouk K, Lucey AD (1999) A theoretical model of pressure propagation in the human spinal CSF system. Eng Mech 6:213–228
7. Chiro GD, Hammock MK, Bleyer WA (1976) Spinal descent of cerebrospinal fluid in man. Neurology 26:1–8
8. Cho KH, Iwasaki YI, Imamura H, Hida K, Abe H (1994) Experimental model of posttraumatic syringomyelia: the role of adhesive arachnoiditis in syrinx formation. J Neurosurg 80:133–139
9. Davis CH, Symon L (1989) Mechanisms and treatment in post-traumatic syringomyelia. Br J Neurosurg 3:669–674
10. Edgar R, Quail P (1994) Progressive post-traumatic cystic and non-cystic myelopathy. Br J Neurosurg 8:7–22
11. Gardner WJ, Angel J (1958) The cause of syringomyelia and its surgical treatment. Cleve Clin Q 25:4–8
12. Gardner WJ, McMurray FG (1976) „Non-communicating'' syringomyelia: a non-existent entity. Surg Neurol 6: 251–256
13. Guizar-Sahagun G, Grijalva I, Madrazo I, Franco-Bourland R, Salgado H, Ibarra A, Oliva E, Zepeda A (1994) Development of post-traumatic cysts in the spinal cord of rats-subjected to severe spinal cord contusion. Surg Neurol 41:241–249
14. Heiss JD, Patronas N, DeVroom HL, Shawker T, Ennis R, Kammerer W, Eidsath A, Talbot T, Morris J, Eskioglu E, Oldfield EH (1999) Elucidating the pathophysiology of syringomyelia. J Neurosurg 91:553–562
15. Ichimura T, Fraser PA, Cserr HF (1991) Distribution of extracellular tracers in perivascular spaces of the rat brain. Brain Res 545:103–113
16. Ikata T, Masaki K, Kashiwaguchi S (1988) Clinical and experimental studies on permeability of tracers in normal spinal cord and syringomyelia. Spine 13:737–741
17. Klekamp J, Batzdorf U, Samii M, Bothe HW (1997) Treatment of syringomyelia associated with arachnoid scarring caused by arachnoiditis or trauma. J Neurosurg 86:233–240
18. Koyanagi I, Tator CH, Lea PJ (1993) Three-dimensional analysis of the vascular system in the rat spinal cord with scanning electron microscopy of vascular corrosion casts. 1. Normal spinal cord. Neurosurgery 33:277–283
19. Lee TT, Alameda GJ, Gromelski EB, Green BA (2000) Outcome after surgical treatment of progressive posttraumatic cystic myelopathy. J Neurosurgery (Spine) 92:149–154
20. Liu D, Thangnipon W, McAdoo DJ (1991) Excitatory amino acids rise to toxic levels upon impact injury to the rat spinal cord. Brain Res 547:344–348
21. Milhorat TH (2000) Classification of syringomyelia. Neurosurg Focus 8:1–6
22. Milhorat TH, Kotzen RM, Anzil AP (1994) Stenosis of central canal of spinal cord in man: incidence and pathological findings in 232 autopsy cases. J Neurosurg 80:716–722
23. Milhorat TH, Capocelli AL Jr, Anzil AP, Kotzen RM, Milhorat RH (1995) Pathological basis of spinal cord cavitation in syringomyelia: analysis of 105 autopsy cases. J Neurosurg 82:802–812
24. Milhorat TH, Capocelli AL Jr, Kotzen RM, Bolognese P, Heger IM, Cottrell JE (1997) Intramedullary pressure in syringomyelia: clinical and pathophysiological correlates of syrinx distension [see comments]. Neurosurgery 41: 1102–1110
25. Oldfield EH, Muraszko K, Shawker TH, Patronas NJ (1994) Pathophysiology of syringomyelia associated with Chiari I malformation of the cerebellar tonsils. Implications for diagnosis and treatment. J Neurosurg 80:3–15
26. Panter SS, Yum SW, Faden AI (1990) Alteration in extracellular amino acids after traumatic spinal cord injury. Ann Neurol 27:96–99
27. Perrouin-Verbe B, Lenne-Aurier K, Robert R, Auffray-Calvier E, Richard I, Mauduyt de la Grève I, Mathe JF (1998) Post-traumatic syringomyelia and post-traumatic spinal canal stenosis: a direct relationship. Review of 75 patients with a spinal cord injury. Spinal Cord 36:137–143
28. Pisharodi M, Nauta HJ (1985) An animal model for neuron-specific spinal cord lesions by the microinjection of N-methylaspartate, kainic acid, and quisqualic acid. Appl Neurophysiol 48: 226–233
29. Rennels ML, Gregory TF, Blaumanis OR, Fujimoto K, Grady PA (1985) Evidence for a 'paravascular' fluid circulation in the mammalian central nervous system, provided by the rapid distribution of tracer protein throughout the brain from the subarachnoid space. Brain Res 326:47–63
30. Rennels ML, Blaumanis OR, Grady PA (1990) Rapid solute transport throughout the brain via paravascular fluid pathways. Adv Neurol 52:431–439
31. Rossier AB, Foo D, Shillito J, Dyro FM (1985) Posttraumatic cervical syringomyelia. Incidence, clinical presentation, electrophysiological studies, syrinx protein and results of conservative and operative treatment. Brain 108: 439–461
32. Schaan M, Jaksche H (2001) Comparison of different operative modalities in post-traumatic syringomyelia: preliminary report. Eur Spine J 10:135–140
33. Schaller B, Mindermann T, Gratzl O (1999) Treatment of syringomyelia after posttraumatic paraparesis or tetraparesis. J Spinal Disord 12:485–488

34. Schurch B, Wichmann W, Rossier AB (1996) Post-traumatic syringomyelia (cystic myelopathy): a prospective study of 449 patients with spinal cord injury. J Neurol Neurosurg Psychiatry 60:61–67
35. Schwartz ED, Yezierski RP, Pattany PM, Quencer RM, Weaver RG (1999) Diffusion-weighted MR imaging in a rat model of syringomyelia after excitotoxic spinal cord injury. Am J Neuroradiol 20:1422–1428
36. Sgouros S, Williams B (1995) A critical appraisal of drainage in syringomyelia. J Neurosurg 82:1–10
37. Simpson RK Jr, Robertson CS, Goodman JC (1990) Spinal cord ischemia-induced elevation of amino acids: extracellular measurement with microdialysis. Neurochem Res 15:635–639
38. Stoodley MA, Jones NR, Brown CJ (1996) Evidence for rapid fluid flow from the subarachnoid space into the spinal cord central canal in the rat. Brain Res 707:155–164
39. Stoodley MA, Gutschmidt B, Jones NR (1999) Cerebrospinal fluid flow in an animal model of noncommunicating syringomyelia. Neurosurgery 44:1065–1075
40. Stoodley MA, Jones NR, Yang LC, Brown CJ (2000) Mechanisms underlying the formation and enlargement of noncommunicating syringomyelia: experimental studies. Neurosurg Focus 8:1–7
41. Wagner FC Jr, VanGilder JC, Dohrmann GJ (1978) Pathological changes from acute to chronic in experimental spinal cord trauma. J Neurosurg 48:92–98
42. Wang D, Bodley R, Sett P, Gardner B, Frankel H (1996) A clinical magnetic resonance imaging study of the traumatised spinal cord more than 20 years following injury. Paraplegia 34:65–81
43. Williams B (1972) Pathogenesis of syringomyelia. Lancet 2:969–970
44. Williams B (1980) On the pathogenesis of syringomyelia: a review. J R Soc Med 73:798–806
45. Williams B (1992) Pathogenesis of post-traumatic syringomyelia. Br J Neurosurg 6:517–520
46. Williams B, Weller RO (1973) Syringomyelia produced by intramedullary fluid injection in dogs. J Neurol Neurosurg Psychiatry 36:467–477
47. Yang L, Jones NR, Stoodley MA, Blumbergs PC, Brown CJ (2001) Excitotoxic model of post-traumatic syringomyelia in the rat. Spine 26:1842–1849
48. Yasui K, Hashizume Y, Yoshida M, Kameyama T, Sobue G (1999) Age-related morphologic changes of the central canal of the human spinal cord. Acta Neuropathol 97:253–259
49. Yezierski RP, Sanata M, Park SH, Madsen PW (1993) Neuronal degeneration and spinal cavitation following intraspinal injections of quisqualic acid in the rat. J Neurotrauma 10:445–456